

An insight of p-type to n-type conductivity conversion in oxygen ion-implanted ultrananocrystalline diamond films by impedance spectroscopy

Hui Xu^{1, 2}, Haitao Ye^{2, a)}, David Coathup², Ivona Z. Mitrovic³, Ayendra D. Weerakkody³, Xiaojun Hu^{1, b)}

- 1. College of Materials Science and Engineering, Zhejiang University of Technology, Hangzhou, China*
- 2. School of Engineering and Applied Science, Aston University, Birmingham B4 7ET, United Kingdom*
- 3. Department of Electrical Engineering and Electronics, University of Liverpool, Liverpool L69 3GJ, United Kingdom*

a) Electronic email: h.ye@aston.ac.uk

b) Electronic email: huxj@zjut.edu.cn

The impedance spectroscopy measurements were used to investigate the separated contributions of diamond grains and grain boundaries (GBs), giving an insight of p-type to n-type conductivity conversion in O⁺-implanted ultrananocrystalline diamond (UNCD) films. It is found that both diamond grains and GBs promote the conductivity in O⁺-implanted UNCD films, in which GBs make at least half contribution. The p-type conductivity in O⁺-implanted samples is a result of H-terminated diamond grains, while n-type conductive samples is closely correlated to O-terminated O⁺-implanted diamond grains and GBs in the films. The results also suggest that low resistance of GBs is preferable to obtain high mobility n-type conductive UNCD film.

Diamond is a promising material as a semiconductor for the fabrication of high performance electronic devices. The diamond p-n junction is a fundamental basic component to fabricate electronic devices. However, the preparation of high-quality shallow-donor n-type diamond remains a challenging task. Many researchers have studied dopants including nitrogen, sulfur, oxygen and phosphorous inserted into single or polycrystalline diamond by ion-implantation or growth during chemical vapour deposition (CVD) process.¹⁻³ Substitutional nitrogen acted as donors that caused electrical conduction with an activation energy of ≈ 1.7 eV in natural diamond, which was too high for room-temperature activation.⁴ Studies on diamond-containing phosphorous donors showed that the activation energy for conduction was 0.4-0.6 eV.^{2,5-8} Room-temperature mobility up to ~ 660 $\text{cm}^2\text{V}^{-1}\text{s}^{-1}$ for a single crystal diamond film with a phosphorus concentration of 7×10^{16} cm^{-3} was achieved.⁶ Inversion channel metal-oxide-semiconductor field-effect transistors were recently fabricated based on phosphorus-doped diamond.⁹ However, the carriers provided to the conduction band by phosphorus ionization is very limited at low doping concentrations. At room temperature the ionization level is only 10^{-5} - 10^{-6} .¹⁰ Heavy P-doping technique was needed to induce hopping conduction, which increased the density of free carriers at room temperature for device fabrication such as junction field-effect transistors.¹¹⁻¹³ With a high dopant concentration above $\sim 10^{20}$ cm^{-3} , the conduction mechanism is described as hopping conduction with activation energy in the order of 0.05 eV as shown by Kato *et al.*¹⁴

Ultrananocrystalline diamond (UNCD) film has a unique microstructure composed of nanocrystalline diamond and grain boundaries (GBs) with potential n-type doped properties. It was reported that nitrogen doped UNCD film exhibits n-type conductivity with the mobility of 1-5 $\text{cm}^2\text{V}^{-1}\text{s}^{-1}$ and activation energy below 10 meV.¹⁵ This conductivity was due to the manipulation of the nanostructure of the material, leading to the enhanced sp^2 regions and midgap states in GBs.¹⁶ Theoretical modelling also showed that nitrogen promoted π bonded states within the GBs, resulting in an impurity band near the Fermi level.¹⁷ It was suggested that nitrogen induced percolated paths in the GB regions and therefore increases the n-type conductivity.¹⁸ Lithium was also reported to enhance n-type conductivity in UNCD films by promoting the formation of disordered carbon nanochannels in GBs.¹⁹ However, the high conductivity was required at the cost of mobilities due to the disordered nature of UNCD films.¹⁶ The nitrogen or lithium atoms tend to be located at GBs during

CVD process, seldomly incorporated into diamond grains, thus diamond grains are likely to be highly resistive in UNCD films.

Once impurity atoms are incorporated into diamond by non-equilibrium events such as ion-implantation, such atoms would prefer to induce defects in diamond grains, which will supply a conductive path along diamond grains in UNCD films. Our previous work prepared both p-type and n-type conductive UNCD films by O ion implantation.²⁰ A novel conduction model was proposed that O⁺-implanted diamond grains supplied n-type conductivity, while GBs gave a current path to the UNCD films.²⁰ However, there is no direct evidence neither to distinguish the contributions of diamond grains and GBs to the conductivity of these films nor to give the insight of conductivity transformation from p-type to n-type.

Impedance spectroscopy (IS) has been widely utilized to study the conduction paths within a range of conductive and less conductive materials.^{21,22} Its strength lies in the ability to identify the individual components contributing to the overall conductivity. It has also been used to characterize the conduction paths in polycrystalline, nanocrystalline diamond films and diamond MOS structures at various biases.²³⁻²⁷ Here, IS and temperature dependent current-voltage (I-V) technique were used to understand the conduction mechanism and obtain the inherent insight of conductivity transition in O⁺-implanted UNCD films. This has significance in the preparation of nanocrystalline diamond based devices.

UNCD films were deposited by a hot filament CVD system on single crystal silicon (111) wafers. The as-deposited UNCD films were treated as substrates where O ion implantation was performed at room temperature with 90 keV and dose of 10^{12} cm⁻².²⁰ For room-temperature implantation, there existed a universal critical damage density, 10^{22} vacancies/cm³, which, when exceeded, resulted in the complete graphitization of heavily damaged diamond crystals upon annealing.²⁸ It was reported that the critical dose of O ion implantation was 10^{16} cm⁻² at room temperature with dose energy of 90 keV in UNCD films²⁹, which means the damage caused by ion implantation in this work can be annealed back after annealing. The implanted samples were annealed at 500, 650, 725, 800, 900, 1000 °C for 30 min with the pressure of 4000 Pa (80% N₂ and 20% O₂),²⁰ named as O12500, O12650, O12725, O12800, O12900 and O121000, respectively. The annealing at 900 °C for 30 min was performed on as-deposited UNCD film (sample 900-A) to analyse the role of annealing on the electrical properties of UNCD films. Ti (500 nm)/Au (300 nm) contacts were made on the surface of films and I-V measurements at room temperature showed that ohmic-contacts formed. Hall effects measurements were performed on the samples on the Accent HL5500

Hall system. The impedance properties of samples were determined using AUTOLAB potentiostatgalvanostat connected with a four-probe station covering the frequency range from 0.01 Hz to 10 MHz. The distance between electrodes was kept constant at 2 mm to obtain comparable results. Temperature dependent I-V measurements were carried out by Agilent B1500A Semiconductor Device Analyzer.

The Hall effect measurement results of samples are listed in Tab. 1. It shows that the as-deposited sample is p-type conductive while it becomes n-type conductive after 900 °C annealing with Hall mobility values increasing from 17.6 to 31.3 cm²V⁻¹s⁻¹. In O⁺-implanted samples, the conductivity changes from p-type to n-type as annealing temperature (T_a) increasing above 800 °C. The Hall mobility values are in the range of 1-18 cm²V⁻¹s⁻¹ in p-type conductive samples and 4-126 cm²V⁻¹s⁻¹ in n-type samples.

IS measurements were carried out to explore the insight into the conductivity transition from p-type to n-type. The cross-section of the fabricated device is shown in Fig. 1(a), and a double resistance-capacitance (RC) parallel model in series was used to simulate the electrical conduction contribution from diamond grains and GBs, as illustrated in Fig. 1(b). The resistance between the electrode and diamond films was taken into account during practical measurements, here defined as R_e. Each parallel RC equivalent circuit model fitted each Cole-Cole semicircle accurately. The fitting procedure used here was the same as the one described by Kleitz and Kennedy and allowed the determination of resistance and relaxation frequencies with a good precision.³⁰ Here the symbols R_g, R_b, C_g, C_b represent the resistance (R) and capacitance (C) of diamond grains and GBs, respectively. The impedance as a complex number, is expressed in supplementary materials.

Fig. 2(a) shows the Bode plots measured for the silicon substrate, as-deposited sample, sample 900-A and O12 series samples. The low frequency impedance value of the silicon substrate is lower than 10³ Ω, which means the effect of current condition through the silicon substrate on the measured resistance was estimated to be less than 1 % over the frequency range and thus could be ignored, as a similar assumption has been used previously by others.^{31,32} It is observed that the impedance values of all samples gradually decrease with frequency increasing. They are nearly the same at high frequency, meaning that the conductive behaviour in this region is quite similar in these samples. The low frequency impedance values of O12 series samples, sample 900-A and as-deposited sample are in the range of 10⁴-10⁵ Ω, which are several orders of magnitude smaller than those of nanocrystalline diamond films (10⁶ Ω),²⁶ detonation nanodiamonds (10⁹ Ω)³³ and

phosphorus-doped single crystalline diamond film ($10^9 \Omega$)³⁴ at room temperature. This means that UNCD films are more conductive.

Specifically, the low impedance value of as-deposited sample is 28 k Ω . It increases to 40 k Ω in sample O12500 and decreases to 20 k Ω in sample O12650. As T_a increases from 650 to 900 °C, it gradually increases and reaches 45 k Ω in sample O12900. It is observed that the values of samples O12900 and O121000 are close to each other, and they are the highest among these samples. Note that the impedance value of sample O12500 is higher than that of sample O12800 at low frequency, while it becomes lower as frequency increases. This also indicates that there are at least two components participating in the conductivity. It is found that the low impedance values of p-type conductive O⁺-implanted UNCD films tend to be lower than those of n-type conductive UNCD films. As the microstructure of nanocrystalline diamond grains and GBs inevitably change at different T_a , the total impedance are required to be resolved into more refined data to analyse the contribution of each part.

Fig. 2(b) shows the characteristic Cole-Cole plots measured for O12 series samples, sample 900-A and as-deposited sample in the whole frequency range of 100 Hz-10 MHz. It is observed that the semicircular response in sample O12500 is accompanied by an additional semicircle which extends to low frequencies, in which high frequency response is incomplete and measured as an arc due to the limited measuring range. There are also two semicircles extracted in the samples except for sample O12900, indicating that there exists two conductive paths. However, for sample O12900, one semicircle means that one conductive path plays a dominant role in the conductivity.

In order to understand the responses quantitatively, the resistance and capacitance values were extracted according to the double RC parallel model shown in Fig. 1(a) and listed in Table 2. It can be seen that the semicircular response at low frequency displays a capacitance value in the range of 1-9 nF, whereas the high frequency region has a capacitance of 70-110 pF. For polycrystalline materials, it is well-established that capacitance values in picofarad levels arise from the contribution to the impedance measurement from crystal grains, while nanofarad level responses can be attributed to GBs.³⁵ It is therefore clear that both nanocrystalline diamond grains and GBs in UNCD films contribute to the electrical characteristics being measured.

The R_e values listed in Table 2 remain in 1.4-1.7 k Ω , which means that the ohmic contact is stable in these samples, as well as the good condition of testing. It is observed that the R_g value of as-deposited sample is 25.9 k Ω , and it significantly decreases to 4.5 k Ω in

sample 900-A. This implies that 900 °C annealing decreases the resistance of diamond grains in UNCD films. After O ions implantation, the R_g values of samples O12500, O12650, and O12725 decrease to 19.4, 15.7 and 24.9 k Ω compared to that of as-deposited sample, respectively. With T_a increasing to 800, 900 and 1000 °C, R_g values dramatically increase to 29.2, 44.6 and 30.4 k Ω , respectively. It is found that low-impedance nanocrystalline diamond grains give more contribution to p-type conductive O⁺-implanted UNCD films while high-impedance grains promote n-type conductive films. Note that sample 900-A also exhibits n-type conduction despite the low impedance value of diamond grains, indicating there is another factor promoting n-type conductivity.

Table 2 shows that the R_b values are much lower than those of R_g in all these samples, indicating GBs are more conductive than diamond grains in UNCD films. The R_b value of sample 900-A is 2.2 k Ω , slightly higher than 1.4 k Ω in as-deposited sample. It reveals that annealing mainly decreases the impedance of diamond grains rather than GBs. The R_b value of sample O12500 increases to 19.2 k Ω , close to the R_g value, which means diamond grains and GBs almost make the equal contribution to the conductivity. Also, the R_b value of sample O12500 is much higher than that of as-deposited sample, indicating that the GBs become more resistive. This is probably because of the imperfection induced by ion bombardment which cannot be recovered at low temperature annealing. The R_b values are 2.8, 2.8, 7.6, 13.0 k Ω in samples O12650, O12725, O12800 and O121000, respectively. The resistance of GBs is too low to be detected compared to diamond grains in sample O12900, meaning that its GBs are very conductive. Our previous work²⁰ showed that graphene nanoribbons formed in GBs of samples 900-A and O12900 (much more formed in sample O12900), making GBs a highly conductive network. When T_a reaches 1000 °C, the conductive GB network was destroyed by higher temperature annealing,²⁰ leading to the increase of the impedance of GBs.

The ratio of R_g to R_b (R_g/R_b) value is calculated and listed in Table 2 to estimate the conductivity contribution in UNCD films. This value for as-deposited sample is 18.5, the highest among these samples, which means the GBs make the largest contribution. It dramatically decreases to 2.0 for sample 900-A, indicating that the contribution of diamond grains sharply increases. In samples O12500, O12650 and O12725, the R_g/R_b values are 1.0, 5.6 and 8.9, respectively, which are lower than that of as-deposited sample. The contribution of diamond grains to conductivity is increased by both diamond grains themselves and higher resistances of GBs, while it is resulted from the increasing resistances of GBs in sample O12800. It is observed that the value for sample O12900 is undetectable because of the low

impedance of GBs compared to diamond grains. This implies that GBs make majority contribution to the conductivity. The R_g/R_b value for samples O121000 is 2.3, indicating that diamond grains provide more support in the conductivity when the nanoribbon network is destroyed.

The impedance results show that both diamond grains and GBs contribute to the conductivity in O^+ -implanted samples, in which GBs are more active. The contribution of diamond grains increases after implantation and annealing, except for sample O12900. It is found that the resistances of diamond grains in p-type conductive samples are lower than those in n-type conductive samples, which means low resistance of diamond grains promotes p-type conductivity while high resistance promotes n-type conductivity in O^+ -implanted UNCD films. It is also observed that the mobility value of sample 900-A is an order of magnitude lower than that of sample O12900, which is consistent with the resistance of diamond grains. The contribution of diamond grains also relies on the resistance of GBs in each sample, because the resistances of GBs vary after different temperature annealing. It is noted that the Hall mobility values for sample O12900 is $126 \text{ cm}^2\text{V}^{-1}\text{s}^{-1}$, which is much higher than those of p-type samples ($1\text{-}18 \text{ cm}^2\text{V}^{-1}\text{s}^{-1}$). This indicates that conductive GBs help increase mobility values in n-type UNCD films more effectively than in p-type UNCD films. This is in agreement with that mobility in sample 900-A is higher than that in as-deposited sample. The mobility value is still low in samples O12800 and O121000, where the resistances of GBs are much higher than that of sample O12900.

Many researchers reported that H-terminated diamond was conductive while O-terminated diamond was insulating.³⁶⁻³⁸ The O-terminated diamond surface vanished after $400 \text{ }^\circ\text{C}$ annealing in vacuum.³⁹ While Thomas Lechleitner *et al.*⁴⁰ oxidized nanocrystalline diamond films by thermal post-processing at $400 \text{ }^\circ\text{C}$ with 21 % oxygen rendering, resulting in the O-termination of nanocrystalline diamond films. These results show that the status of O-terminated diamond surface heavily depends on the annealing atmosphere. Unlike the oxygen desorption behaviour annealed in vacuum, samples in this work were annealed in quartz tube with limited air remaining and XPS results proved that the surface of diamond grains gradually changed from H-terminated to O-terminated as T_a increases in O^+ -implanted samples.²⁰ (See supplementary materials Figure S1) As one of the source gases during CVD process, hydrogen makes the diamond grains H-terminated and such surface induces p-type surface conductivity.⁴¹ This is in agreement with impedance measurement results, where the nanocrystalline diamond grains in p-type are more conductive than those in n-type O^+ -

implanted films. The surface of diamond grains in O⁺-implanted UNCD films is oxidized to be O-terminated when T_a is above 800 °C, making the R_g value higher than that of as-deposited sample. This suggests that the transition of p-type conductivity to n-type in O⁺-implanted samples when T_a increases from 725 to 800 °C is closely correlated to the diamond grains.

It had also been reported that the H-terminated surface was irreversibly destroyed after 750 °C and above temperature annealing.⁴² Hydrogen bonding to the diamond grain surface and GBs in nanodiamond films was stable up to elevated temperatures of ~800 °C and then decomposed at higher temperatures.⁴³ This is in consistent with IS result that H-terminated diamond surface changes to O-terminated in the T_a range of 725-800 °C. The H-terminated diamond surface had localized surface states in the band gap which would comprise the electron conductivity in n-type doping as they were expected to act as electron traps.⁴⁴ The dramatically reduced value of the resistance of diamond grains in sample 900-A reveals the surface change of grains after 900 °C annealing. The energy band structure at the surface of oxidized UNCD films showed a large density of states within the expected diamond band gap resulting from sp² carbon in the GBs or other surface states related to the termination. This suggests that GBs also play an important role in the conductivity transition when hydrogen bondings decomposed from diamond grains. π-bonded states originated from GBs were reported to be responsible for the n-type conductivity in N-doped UNCD films with an activation energy below 10 meV.¹⁵ As the measuring temperature increases to 400 °C, the corresponding activation energy increases to 0.05-0.15 eV.⁴⁵ It is likely that p-type conductivity is induced by the H-terminated diamond grains, while GBs induce n-type conductivity after hydrogen bondings decomposed at higher annealing temperature, which explains the p-type to n-type conductivity conversion from as-deposited sample to sample 900-A. However, oxygen also induced an n-type conductive layer with an activation energy of about 0.32 eV in single crystalline diamond by ion implantation.⁴⁶ It is thus not clear whether GBs or oxygen ions induce n-type conductivity in samples O12900 and O121000.

Temperature dependant I-V measurements were carried out to estimate the activation energy of samples O12650, O12900, 900-A and as-deposited sample, as shown in Fig. 3. The activation energy values for these samples are 0.10 eV, 0.11 eV, 0.04 eV and 0.11 eV, respectively. The activation energy of H-terminated surface conductivity is 3-20 meV in single and polycrystalline diamond films,⁴⁷ which is much lower than those of as-deposited sample and sample O12650. Ohmagariet *et al.*⁴⁸ reported an activation energy of about 0.1

eV in B-doped p-type conductive UNCD films, in which conduction mechanism remains unknown. The activation energy of H-terminated diamond grains is too low compared to overall activation energy of the film. While for the n-type conductive samples, the activation energy of sample 900-A is 0.04 eV, which is lower than that of sample O12900, indicating the mechanism of n-type conductivity is different. As the H-terminated diamond surface destroyed and graphene nanoribbons formed in sample 900-A, π -bonded states originated from GBs are responsible for the n-type conductivity. The activation energy of sample O12900 is lower than 0.32 eV but higher than 0.04 eV, which can be regarded as the combination of π -bonded states and O-terminated diamond promoting n-type conduction together. The oxygen ions make diamond grains activated in n-type conduction when T_a is above 800 °C, where the transportation of electrons largely relies on the conductivity of GBs. In this way, samples annealed at 900 °C, which have lower impedance values of GBs than those samples annealed at 800 and 1000 °C, form a conductive network of electrons to obtain high mobility n-type UNCD films.

In summary, the impedance spectroscopy results directly evidence the contributions of both diamond grains and GBs to the conductivity, and give an insight of conductivity transformation from p-type to n-type in O^+ -implanted UNCD films. The results show that GBs make at least half contribution. The p-type conductivity in O^+ -implanted samples is resulted from H-terminated diamond grains, while n-type conductive samples has a close relation to O-terminated O^+ -implanted diamond grains and GBs in the UNCD films. The results also suggest that low resistance of GBs is preferable to obtain high mobility n-type conductive UNCD films. These UNCD films have applications in electrochemical electrodes, field emission, heterostructures, high-temperature stable ohmic contacts and ion-sensitive field-effect transistor in harsh environment.

Supplementary material

See supplementary material for the complex impedance and XPS results of samples.

Acknowledgment

This work was supported by the National Natural Science Foundation of China (Grant Nos. 50972129 and 50602039) and by the international science technology cooperation program of

China (2014DFR51160). The work was also supported by European Union FP7 Marie Curie Action (Project No 295208) and Horizon 2020 Action (Project No 734578).

References

- ¹ I. Sakaguchi, M. N.-Gamo, Y. Kikuchi, E. Yasu, H. Haneda, T. Suzuki, and T. Ando, *Phys. Rev. B* **60** (4), R2139 (1999).
- ² S. Koizumi, T. Teraji, and H. Kanda, *Diamond Relat. Mater.* **9** (3–6), 935 (2000).
- ³ R. Ohtani, T. Yamamoto, S. D. Janssens, S. Yamasaki, and S. Koizumi, *Appl. Phys. Lett.* **105** (23), 232106 (2014).
- ⁴ R. Farrer, *Solid State Commun.* **7** (9), 685 (1969).
- ⁵ S. Koizumi, M. Kamo, Y. Sato, H. Ozaki, and T. Inuzuka, *Appl. Phys. Lett.* **71**, 1065 (1997).
- ⁶ M. Katagiri, J. Isoya, S. Koizumi, and H. Kanda, *Appl. Phys. Lett.* **85** (26), 6365 (2004).
- ⁷ S. Koizumi, M. Kamo, Y. Sato, S. Mita, A. Sawabe, A. Reznik, C. Uzan-Saguy, and R. Kalish, *Diamond Relat. Mater.* **7** (2), 540 (1998).
- ⁸ S. Koizumi, *Phys. Status Solidi A* **172** (1), 71 (1999).
- ⁹ T. Matsumoto, H. Kato, K. Oyama, T. Makino, M. Ogura, D. Takeuchi, T. Inokuma, N. Tokuda, and S. Yamasaki, *Scientific Reports* **6** (2016).
- ¹⁰ T. A. Grotjohn, D. T. Tran, M. K. Yaran, S. N. Demlow, and T. Schuelke, *Diamond Relat. Mater.* **44**, 129 (2014).
- ¹¹ H. Kato, H. Umezawa, N. Tokuda, D. Takeuchi, H. Okushi, and S. Yamasaki, *Appl. Phys. Lett.* **93** (20), 202103 (2008).
- ¹² K. Oyama, S.-G. Ri, H. Kato, M. Ogura, T. Makino, D. Takeuchi, N. Tokuda, H. Okushi, and S. Yamasaki, *Appl. Phys. Lett.* **94** (15) (2009).
- ¹³ M. Kasu, K. Ueda, Y. Yamauchi, A. Tallaire, and T. Makimoto, *Diamond Relat. Mater.* **16** (4), 1010 (2007).
- ¹⁴ H. Kato, D. Takeuchi, N. Tokuda, H. Umezawa, H. Okushi, and S. Yamasaki, *Diamond Relat. Mater.* **18** (5–8), 782 (2009).
- ¹⁵ O. A. Williams, S. Curat, J. E. Gerbi, D. M. Gruen, and R. B. Jackman, *Appl. Phys. Lett.* **85** (10), 1680 (2004).
- ¹⁶ O. A. Williams, *Semicond. Sci. Technol.* **21** (8), R49 (2006).
- ¹⁷ P. Zapol, M. Sternberg, L. A. Curtiss, T. Frauenheim, and D. M. Gruen, *Phys. Rev. B* **65** (4), 045403 (2001).
- ¹⁸ S. Bhattacharyya, *Phys. Rev. B* **70** (12), 125412 (2004).
- ¹⁹ P. T. Joseph, N. H. Tai, and I. N. Lin, *Appl. Phys. Lett.* **97** (4) (2010).
- ²⁰ X. Hu, C. Chen, and S. Lu, *Carbon* **98**, 671 (2016).
- ²¹ A. Huanosta and A. West, *J. Appl. Phys.* **61** (12), 5386 (1987).
- ²² N. Hirose and A. R. West, *J. Am. Ceram. Soc.* **79** (6), 1633 (1996).
- ²³ H. Ye, O. Gaudin, R. Jackman, P. Muret, and E. Gheeraert, *Phys. Status Solidi A* **199** (1), 92 (2003).
- ²⁴ H. Ye, C. Q. Sun, H. Huang, and P. Hing, *Thin Solid Films* **381** (1), 52 (2001).
- ²⁵ H. Ye, O. A. Williams, R. Jackman, R. Rudkin, and A. Atkinson, *Phys. Status Solidi A* **193** (3), 462 (2002).
- ²⁶ M. Bevilacqua, N. Tumilty, C. Mitra, H. Ye, T. Feygelson, J. E. Butler, and R. B. Jackman, *J. Appl. Phys.* **107** (3), 033716 (2010).
- ²⁷ M. Liao, J. Liu, L. Sang, D. Coathup, J. Li, M. Imura, Y. Koide, and H. Ye, *Appl. Phys. Lett.* **106** (8), 083506 (2015).
- ²⁸ C. Uzan - Saguy, C. Cytermann, R. Brener, V. Richter, M. Shaanan, and R. Kalish, *Appl. Phys. Lett.* **67** (9), 1194 (1995).
- ²⁹ X. J. Hu, J. S. Ye, H. J. Liu, Y. G. Shen, X. H. Chen, and H. Hu, *J. Appl. Phys.* **109** (5), 053524 (2011).

- ³⁰ M. Kleitz, J. Kennedy, P. Vashishta, J. Mundy, and G. Shenoy, Noth Holland: Elsevier, 185 (1979).
- ³¹ M. Koichi and L. D. David Jpn. J. Appl. Phys. **33** (8R), 4526 (1994).
- ³² H. Ye, O. Gaudin, R. B. Jackman, P. Muret, and E. Gheeraert, Phys. Status Solidi **199** (1), 92 (2003).
- ³³ M. Bevilacqua, S. Patel, A. Chaudhary, H. Ye, and R. B. Jackman, Appl. Phys. Lett. **93** (13), 2115 (2008).
- ³⁴ S. Curat, H. Ye, O. Gaudin, R. B. Jackman, and S. Koizumi, J. Appl. Phys. **98** (7), 073701 (2005).
- ³⁵ J. R. McDonald, Impedance Spectroscopy Emphasizing Solid Materials and Systems (1987).
- ³⁶ J. C. Piñero, D. Araújo, A. Fiori, A. Traoré, M. P. Villar, D. Eon, P. Muret, J. Pernot, and T. Teraji, Appl. Surf. Sci.
- ³⁷ T. Sakai, K.-S. Song, H. Kanazawa, Y. Nakamura, H. Umezawa, M. Tachiki, and H. Kawarada, Diamond Relat. Mater. **12** (10), 1971 (2003).
- ³⁸ D. A. Moran, S. A. Russell, S. Sharabi, and A. Tallaire, presented at the Nanotechnology (IEEE-NANO), 2012 12th IEEE Conference on, 2012 (unpublished).
- ³⁹ P. Muret, A. Traoré, A. Maréchal, D. Eon, J. Pernot, J. Pinéro, M. d. P. Villar, and D. Araujo, Journal of Applied Physics **118** (20), 204505 (2015).
- ⁴⁰ T. Lechleitner, F. Klauser, T. Seppi, J. Lechner, P. Jennings, P. Perco, B. Mayer, D. Steinmüller-Nethl, J. Preiner, and P. Hinterdorfer, Biomaterials **29** (32), 4275 (2008).
- ⁴¹ F. Maier, M. Riedel, B. Mantel, J. Ristein, and L. Ley, Phys. Rev. Lett. **85** (16), 3472 (2000).
- ⁴² S. Q. Lud, M. Niedermeier, P. S. Koch, P. Bruno, D. M. Gruen, M. Stutzmann, and J. A. Garrido, Appl. Phys. Lett. **96** (9), 092109 (2010).
- ⁴³ S. Michaelson, A. Stacey, J. Orwa, A. Cimmino, S. Prawer, B. Cowie, O. A. Williams, D. Gruen, and A. Hoffman, J. Appl. Phys. **107** (9), 093521 (2010).
- ⁴⁴ S. J. Sque, R. Jones, and P. R. Briddon, Phys. Rev. B **73** (8), 085313 (2006).
- ⁴⁵ M. Mertens, M. Mohr, N. Wiora, K. Brühne, and H.-J. Fecht, J. Nanomater **2015**, 3 (2015).
- ⁴⁶ J. F. Prins, Phys. Rev. B **61** (11), 7191 (2000).
- ⁴⁷ C. Sauerer, F. Ertl, C. Nebel, M. Stutzmann, P. Bergonzo, O. A. Williams, and R. Jackman, Phys. Status Solidi A **186** (2), 241 (2001).
- ⁴⁸ S. Ohmagari, T. Yoshitake, A. Nagano, R. Ohtani, H. Setoyama, E. Kobayashi, T. Hara, and K. Nagayama, Jpn. J. Appl. Phys. **49** (3R), 031302 (2010).

Table 1 The Hall effects values of as-deposited sample, sample 900-A, and O12 series samples annealed at different temperatures ²⁰

Sample	Sheet resistance ($10^4 \Omega/\text{square}$)	Hall coefficient (m^2C^{-1})	Hall mobility ($\text{cm}^2\text{V}^{-1}\text{s}^{-1}$)	Sheet carrier concentration (10^{13}cm^{-2})
As-deposited	2.24	39.5	17.6	1.58
900-A	0.66	-20.6	31.3	-3.03
O12500	1.31	9.91	7.56	6.29
O12650	2.30	2.45	1.07	25.4
O12725	2.83	11.50	4.08	5.41
O12800	3.55	-16.30	4.58	-3.84
O12900	1.28	-162	126	-0.386
O121000	2.43	-19.10	7.86	-3.27

Table 2 Resistance and capacitances values of O⁺-implanted UNCD films fitted from impedance spectroscopy

Sample	R _e (kΩ)	R _g (kΩ)	C _g (pF)	R _b (kΩ)	C _b (nF)	R _g /R _b
As-deposited	1.4	25.9	71.4	1.4	2.2	18.5
900-A	1.5	4.5	105.0	2.2	7.5	2.0
O12500	1.5	19.4	78.4	19.2	1.7	1.0
O12650	1.4	15.7	74.9	2.8	1.5	5.6
O12725	1.5	24.9	72.0	2.8	5.8	8.9
O12800	1.6	29.2	79.5	7.6	3.9	3.8
O12900	1.5	44.6	68.4	-	-	-
O121000	1.7	30.4	94.3	13.0	8.3	2.3

Figure captions:

Fig. 1 (a) Schematic diagram of the cross-section of the sample. (b) Equivalent circuit for the electrical response of a UNCD sample with contributions from diamond grains (g) and grain boundaries (b), and the electrode interface (e).

Fig. 2 (Color online) (a) Bode plots measured for as-deposited sample, sample 900-A and O12 series samples. (b) The characteristic Cole-Cole plots measured for as-deposited sample, sample 900-A and O12 series samples.

Fig. 3 (Color online) Temperature dependence of resistance from I-V measurement of as-deposited sample, samples 900-A, O12650 and O12900. Linear curve fitting from 20-100 °C shows activation energy values are 0.11 eV, 0.04 eV, 0.10 eV and 0.11 eV, respectively.

Fig. 1

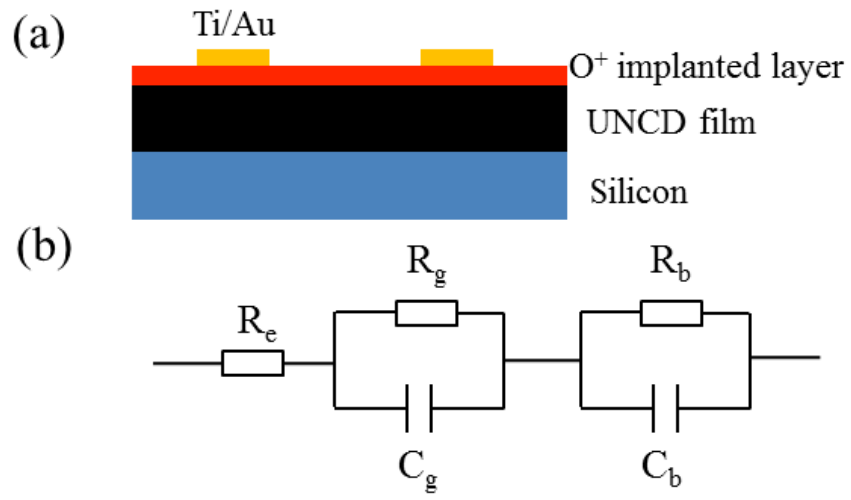


Fig. 2

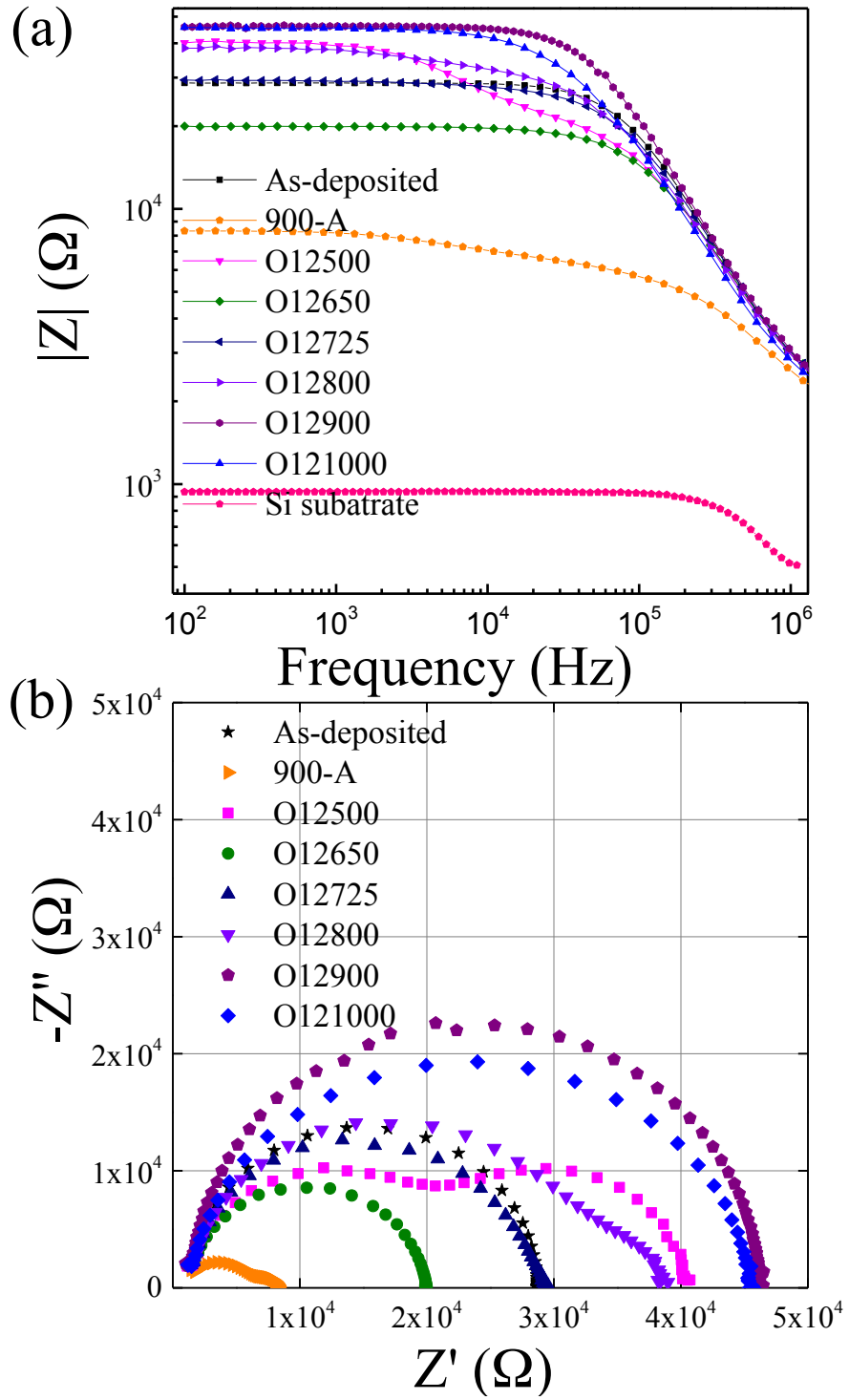


Fig. 3

